

## Spike detection and clustering with unsupervised wavelet optimization in extracellular neural recordings

Shalchyan, Vahid; Jensen, Winnie; Farina, Dario

*Published in:*  
I E E E Transactions on Biomedical Engineering

*DOI (link to publication from Publisher):*  
[10.1109/TBME.2012.2204991](https://doi.org/10.1109/TBME.2012.2204991)

*Publication date:*  
2012

*Document Version*  
Accepted author manuscript, peer reviewed version

[Link to publication from Aalborg University](#)

*Citation for published version (APA):*  
Shalchyan, V., Jensen, W., & Farina, D. (2012). Spike detection and clustering with unsupervised wavelet optimization in extracellular neural recordings. *I E E E Transactions on Biomedical Engineering*, 59(9), 2576-2585. <https://doi.org/10.1109/TBME.2012.2204991>

### General rights

Copyright and moral rights for the publications made accessible in the public portal are retained by the authors and/or other copyright owners and it is a condition of accessing publications that users recognise and abide by the legal requirements associated with these rights.

- Users may download and print one copy of any publication from the public portal for the purpose of private study or research.
- You may not further distribute the material or use it for any profit-making activity or commercial gain
- You may freely distribute the URL identifying the publication in the public portal -

### Take down policy

If you believe that this document breaches copyright please contact us at [vbn@aub.aau.dk](mailto:vbn@aub.aau.dk) providing details, and we will remove access to the work immediately and investigate your claim.



# Spike Detection and Clustering with Unsupervised Wavelet Optimization in Extracellular Neural Recordings

Vahid Shalchyan, *Student Member, IEEE*, Winnie Jensen, *Member, IEEE*, and Dario Farina\*, *Senior Member, IEEE*

**Abstract**—Automatic and accurate detection of action potentials of unknown waveforms in noisy extracellular neural recordings is an important requirement for developing brain-computer interfaces. This study introduces a new, wavelet-based manifestation variable that combines the wavelet shrinkage denoising with multi-scale edge detection for robustly detecting and finding the occurrence time of action potentials in noisy signals. To further improve the detection performance by eliminating the dependence of the method to the choice of the mother wavelet, we propose an unsupervised optimization for best basis selection. Moreover, another unsupervised criterion based on a correlation similarity measure was defined to update the wavelet selection during the clustering to improve the spike sorting performance. The proposed method was compared to several previously proposed methods by using a wide range of realistic simulated data as well as selected experimental recordings of intra-cortical signals from freely moving rats. The detection performance of the proposed method substantially surpassed previous methods for all signals tested. Moreover, updating the wavelet selection for the clustering task was shown to improve the classification performance with respect to maintaining the same wavelet as for the detection stage.

**Index Terms**—Action potential, extracellular recording, spike detection, spike sorting, unsupervised optimization, wavelet design.

## I. INTRODUCTION

EXTRACELLULAR recordings from neuronal activities of the brain can be used as a source of information for brain-computer interfacing (BCI). Decoding the discharge pattern of several neurons allows prediction of the motor output. Microelectrodes can often pick up the action potentials (APs) of a few neurons in a local region near the electrode tip. The signals recorded from these microelectrodes therefore contain

the spike trains from multiple neural units contaminated by background noise. Retrieving the firing information of different units is the main goal of spike sorting techniques. Such information is not only important for studying brain functions but can also be used as an input for BCI applications. The prerequisite for these studies is detecting the APs in the presence of background noise.

The most common method for spike detection is amplitude thresholding which has been often used for real-time implementations of cortically controlled BCI systems [1, 2]. The computational load of this technique is low; however, the procedure is associated with the challenging problem of threshold selection for a trade-off between false negatives and false positives [3]. Methods proposed for the automatic identification of the threshold level [4-6] are based on the estimation of the background noise power and need prior assumption on the noise amplitude distribution (usually Gaussianity). These assumptions are often not verified [7, 8]. Moreover, an inherent problem of the amplitude thresholding methods is that they fail when the spike amplitude peaks are close to or lower than the noise level.

Template matching is another approach for extracting the spikes from noisy background. This approach requires the knowledge on the spike shapes [9, 10]. The detection performance of this method is higher than simple thresholding; however, as a primary step, in order to form the template of different spike morphologies automatically and without any prior knowledge about the signal, another detection algorithm is required which is often based on thresholding [11-13], facing similar issues as outlined above.

The nonlinear energy operator (NEO), magnifies local peaks in both amplitude and frequency, and has been widely used for detecting neural spikes [14, 15]. The NEO spike detection method has been reported to perform well and it is attractive because of its easy implementation and computational simplicity [16]. A modification on the NEO, called the Multi-resolution Teager Energy Operator (MTEO) [17], combines the results of applying the energy operator to the signal with different resolution scales and has shown encouraging results. However, both NEO and MTEO are also threshold-based methods and need manual or automatic level adjustments [18, 19].

Wavelet transformation methods have also been applied for denoising and detection of neural spikes in a noisy environment [8, 20-23]. The main idea behind wavelet based

Manuscript received November 28, 2011. This work was supported in part by a doctoral scholarship from Iran University of Science and Technology, Tehran, Iran. Asterisk indicates corresponding author.

V. Shalchyan is with the Department of Health Science and Technology, Faculty of Medicine, Aalborg University, DK-9220 Aalborg, Denmark, and also with the Department of NeuroRehabilitation Engineering, Bernstein Focus Neurotechnology Göttingen, Bernstein Center for Computational Neuroscience, University Medical Center Göttingen, Georg-August University, Göttingen, Germany (e-mail: vshal@hst.aau.dk).

W. Jensen is with the Department of Health Science and Technology, Faculty of Medicine, Aalborg University, DK-9220 Aalborg, Denmark (e-mail: wj@hst.aau.dk).

\*D. Farina is with the Department of Neurorehabilitation Engineering, Bernstein Focus Neurotechnology Göttingen, Bernstein Center for Computational Neuroscience, University Medical Center Göttingen, Georg-August University, Göttingen, Germany (e-mail: dario.farina@bccn.uni-goettingen.de).

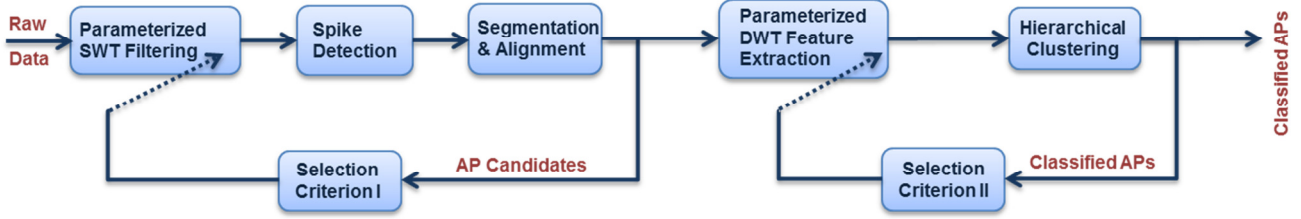


Fig. 1. Block diagram of the proposed method. Criteria I and II based on detected and classified action potential (AP) candidates are used to optimize the wavelet selection in detection and clustering tasks respectively. See text for details.

methods is that using the wavelet transform, the projection of the signal will be localized in the time instants where the signal resembles the mother wavelet shape or its dilated versions in the time-scale domain. Thus, if the mother wavelet shape is selected properly, the wavelet transform can be seen as a bank of matched filters. This implies either an a priori knowledge about the dominant spike shapes or using a procedure for adaptive design of the mother wavelet. Various choices of mother wavelet have been reported for spike detection based on a priori knowledge on the spike shapes, including Daubechies [20], Symlet [22], Coiflet [8], and Biorthogonal [23]. Since there is a significant variability in the AP waveforms in different experimental recordings, due to random positioning of the electrode and the morphology of the neuron [24], there is not a single wavelet optimal for all situations. For this reason, Hulata *et al.* [21] proposed a method for optimal basis selection for the wavelet packet decomposition. However, the method involves a supervised procedure and user intervention in preparing the training dataset for the optimization task. Kamavuako *et al.* [25] proposed an unsupervised algorithm for the selection of the mother wavelet for detection of single unit APs in intrafascicular nerve recordings using a signal-based criterion. This method and many others will be compared to the approach proposed in this study.

In this paper, we propose a new wavelet based method to define a novel manifestation variable for action potential detection. Although the main contribution is on extracellular spike detection, we also describe a hierarchical clustering method that provides a spike sorting of multiunit signals. In addition, two unsupervised optimizations are proposed for mother wavelet selection in the detection and clustering tasks. The method was tested and compared with other approaches by using an extensive set of simulated data as well as selected experimental recording.

## II. METHODS

An overview of the proposed method is shown in Fig.1. The technique consists of two main parts: detection and clustering. Both parts are based on an optimization procedure based on wavelet parameterization. The methods are described in detail in the following.

### A. Stationary Wavelet Transform

The first processing step consists in the stationary wavelet transform (SWT) of the signal. The signal is transformed into

multiple resolution levels by projecting it on a family of scaling  $\phi(t)$  and wavelet  $\psi(t)$  functions. The approximation and the detail coefficients are computed on each scale of decomposition by applying a low-pass filter  $h$  and a high-pass filter  $g$  derived from the scaling and the wavelet basis functions.

Contrary to the discrete wavelet transform (DWT), the SWT does not down-sample the output signal after filtering. Conversely, the discrete filter coefficients are up-sampled at each level. In the case of orthogonal wavelets, the high-pass filter  $g$  can be deduced from the low-pass filter  $h$  through the relation  $g[k] = (-1)^{1-k} \cdot h[1-k]$ , and thus one filter defines the entire decomposition.

### B. Wavelet Parameterization

Since the decomposition and, accordingly, the mother wavelet are completely defined by the scaling filter  $h$ , the parameterization of  $h$  provides a way to describe a family of decompositions and mother wavelets. Filter coefficient parameterization was previously used for different signal processing applications, such as signal classification [26], compression [27], denoising [25], and blind source separation [28]. To generate an orthogonal representation of wavelets in the multi-resolution analysis (MRA) framework,  $h$  must satisfy certain conditions which leave  $L/2 - 1$  free parameters, where  $L$  is the filter length [29, 30]. For  $L = 4$ , the design parameter vector  $\theta = [\alpha]$  is reduced to a scalar parameter:

$$i = 0, 3 \quad h[i] = \frac{1 - \cos(\alpha) + (-1)^i \sin(\alpha)}{2\sqrt{2}} \quad (1)$$

$$i = 1, 2 \quad h[i] = \frac{1 + \cos(\alpha) - (-1)^i \sin(\alpha)}{2\sqrt{2}} \quad (2)$$

In this study, we will use the filter length  $L = 4$ , corresponding to only one independent parameter. This choice reduces the computational time with respect to longer filters and thus may allow the method to be implemented in real-time applications.

### C. Detection

The application of the SWT to a signal contaminated by noise using a mother wavelet matching the spike shapes will result in the signal energy being localized in a few coefficients and the noise spread over several coefficients. This rationale is used in the method of wavelet shrinkage de-noising which is based on coefficient thresholding [31, 32]. Moreover, the

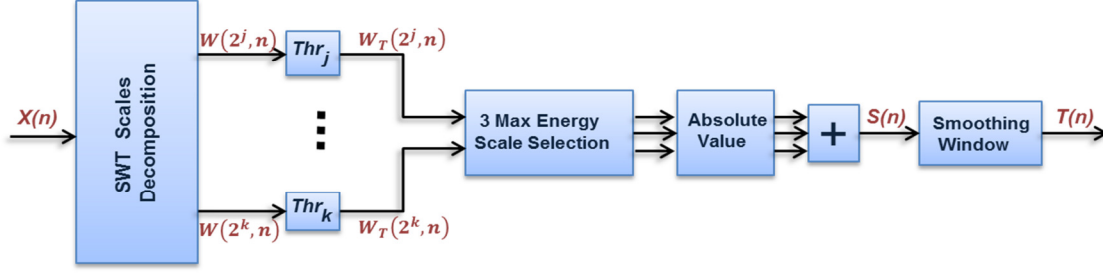


Fig. 2. Block diagram of the proposed method to define a manifestation variable for detection.

detection can be further enhanced by using wavelet multi-scale edge representation [33] and scale multiplication for edge detection [34, 35], as done in image processing. This approach can be generalized to the spike detection by exploiting the fact that the spikes and edges are similar phenomena (i.e., fast signal variations). This approach has been used by Kim & Kim [8] who proposed point-wise product of the wavelet coefficients in three consecutive dyadic scales for calculating a manifestation variable for spike detection. However, the results from a recent simulation study showed weakness of this approach in a wide range of SNRs [18, 19].

We propose a different method to define a manifestation variable for AP detection that combines the wavelet shrinkage denoising with multi-scale edge detection. The method is based on the summation of absolute thresholded coefficients (i.e., after denoising) over the three scales that yield maximum energy. The signal is decomposed over 5 scales by using the parameterized SWT. The coefficients obtained in this way are hard-thresholded to remove the low energy time-scale points in all scales. As in wavelet shrinkage denoising [31], the threshold level at each scale is estimated as follows:

$$Thr_j = \sigma_j \cdot \sqrt{2 \log(N)} \quad (3)$$

where  $N$  is the number of time samples ( $n$ ) and  $\sigma_j$  is the noise standard deviation for the scale  $j$  which is estimated with the median absolute deviation (MAD) operator, as previously proposed [31]:

$$\sigma_j = MAD(W(2^j, n)) / 0.6745 \quad (4)$$

In this study we used 80% of this threshold level to keep the highest 20% as marginal candidates for detection:

$$Thr_j = 0.8 \sqrt{2 \log(N)} \cdot MAD(W(2^j, n)) / 0.6745 \quad (5)$$

Hard thresholding can be described by the following equation, as in [31]:

$$W_T(2^j, n) = \begin{cases} W(2^j, n) & \text{if } |W(2^j, n)| > Thr_j \\ 0 & \text{if } |W(2^j, n)| \leq Thr_j \end{cases} \quad (6)$$

where  $W_T(2^j, n)$  denotes the wavelet coefficients after thresholding at scale  $j$  with threshold level equal to  $Thr_j$ . After hard-thresholding, we select three scales which contain most of the signal energy, assuming that the energy of the noise is distributed approximately equally over all scales. The signal energy at each scale  $EW_j$  is calculated as:

$$EW_j = \sum_{n=1}^N (W_T(2^j, n) - \overline{W_T})^2 \quad (7)$$

where  $W_T(2^j, n)$  is the wavelet coefficient after thresholding at scale  $j$  and  $\overline{W_T}$  denotes the average value at each scale.

Then the manifestation variable  $S(n)$  is calculated as the summation of the absolute values of the thresholded wavelet coefficients over the 3 selected scales:

$$S(n) = \sum_j |W_T(2^j, n)| \quad (8)$$

Finally, for removing spurious peaks,  $S(n)$  is filtered with a Bartlett window of duration equal to half the average length of an action potential, as proposed previously [8]:

$$T(n) = w(n) * S(n) \quad (9)$$

where  $w(n)$  is the Bartlett window used for smoothing and  $T(n)$  is the manifestation variable for detection, and  $*$  denotes convolution. Fig. 2 shows the block diagram of the proposed detection method. Since the selected wavelet scales have been de-noised by hard thresholding, the composed manifestation acts robustly against the detection of false events. Thus no further thresholding is required to prevent such errors and all local peaks of the manifestation with minimum time distance (i.e., between subsequent peaks) of 2 ms are detected as positions of the spikes. For each detected spike, 48 samples were segmented and stored (i.e., 2 ms). All spikes were upsampled by a factor 4 using cubic spline interpolation and aligned to their maximum.

#### D. Wavelet Selection Criterion for Detection

The above detection method can be applied with a parameterized version of the scaling filter (as described in section II-B) for the SWT. By sampling of the parameter  $\alpha$  from 0 to  $2\pi$ ,  $m$  times ( $m=12$ , here) and running the detection procedure for each,  $m$  different variables for detection and consequently  $m$  sets of detected spikes (AP candidates) are generated, among which the best with minimum detection errors should be selected. Detection errors can be false positives (FP) or false negatives (FN). The detection error rate (DER) is defined by the summation of these two types of error, divided by the total number of spikes:

$$DER = \frac{FP + FN}{\text{SpikeNumber}} \% \quad (10)$$

Thus, we define the best mother wavelet as the wavelet that minimizes the metrics DER. However, DER cannot be used in practice for selection of the mother wavelet since it is not known a-priori, thus the best wavelet cannot be directly selected. It is necessary to have a criterion based only on information that can be extracted from the signal. The wavelet resulting from this criterion will be denoted as optimal wavelet and, in the ideal case of perfect criterion, it should correspond to the best wavelet.

We propose a criterion for optimal wavelet selection based on the correlation. We assume that APs recorded from one electrode originating from one or more units are not fully uncorrelated to each other whereas the noise (non-spike event) is uncorrelated to them. Based on this rationale, we define a correlation similarity measure to evaluate the detection performance. The correlation similarity between two waveforms  $x(n)$ ,  $y(n)$  is defined by  $P(x, y)$  as follows:

$$P(x, y) = \frac{E[(x(n) - \mu_x) \cdot (y(n) - \mu_y)]}{\sigma_x \cdot \sigma_y} \quad (11)$$

where  $E$  is the expected value operator,  $\mu_x$ ,  $\mu_y$  are the means and  $\sigma_x$ ,  $\sigma_y$  are the standard deviations of  $x(n)$  and  $y(n)$ , respectively. Based on (11), the correlation between all detected APs,  $AP_i(n)$ , and the median value of them,  $\overline{AP}(n)$ , was calculated and compared to a threshold  $KD$  to classify them into two groups of “reference” and “outliers”, as described in (12):

$$\hat{L}_i = \begin{cases} \text{"reference"} & |P(AP_i, \overline{AP})| \geq KD \\ \text{"outlier"} & |P(AP_i, \overline{AP})| < KD \end{cases} \quad (12)$$

where  $\hat{L}_i$  is the designated label for  $AP_i(n)$ . The threshold value was conservatively set to a low value of  $KD=0.4$  that only rejects very far outliers. The value was determined based on measurements on several experimental neural recordings but not on the experimental dataset used for testing in this study (cases shown in Table I).

The optimal wavelet was chosen among  $m$  wavelets which were generated from the parameterized wavelet as the one leading to the maximum number of *reference* APs. (The wavelet parameterization is demonstrated in section II-B)

### E. Clustering

After the detection, a new parameterized wavelet decomposition is performed for each detected spike as a basis for defining the features for clustering. The DWT is used for this step and the coefficients are extracted from 5 scales. The resulting wavelet coefficients are used as feature vector for the clustering task<sup>1</sup>. The clustering was based on a hierarchical method with normal distance measurement [36, 37] and Ward's Minimum variance method. Ward linkage combines the 2 clusters whose combination results in the smallest increase in the sum of squared deviations from the cluster centroid [36, 37].

### F. Wavelet Selection Criterion for Clustering

The correlation measure described in (11) was applied to evaluate the similarity of each spike to its related cluster center. The identification of the cluster centers was performed by calculating the median of all reference APs for each cluster. Each spike candidate corresponds to a feature vector, computed as described above. All the following computations were done on the feature vectors. For each cluster  $j$ , the correlation of any action potentials ( $AP_{i,j}(n)$ ) with the center

of the cluster  $j$  ( $\overline{AP}_j(n)$ ) was calculated and compared to a threshold value  $KC$ , as described in (13), deciding whether the spikes in each cluster  $j$  are among the inner or outer samples with respect to the center of the clusters. The value for  $KC$  was adjusted empirically to  $KC = 0.8$ , which represents the high similarity requirement for the inner spikes in all clusters:

$$\hat{L}_{i,j} = \begin{cases} \text{"inner"} & P(AP_{i,j}, \overline{AP}_j) \geq KC \\ \text{"outer"} & P(AP_{i,j}, \overline{AP}_j) < KC \end{cases} \quad (13)$$

where  $\hat{L}_{i,j}$  is the designated label for  $AP_{i,j}(n)$ .

The optimal wavelet for clustering was chosen as the one leading to the maximum number of *inner* labeled over all APs.

## III. EVALUATION

### A. Experimental Methods

Experimental recordings of intra-cortical signals from freely moving rats were performed with the recording system TDT RX5 Pentusa Base Station (TDT, Inc.). All experimental procedures were approved by the Animal Experiments Inspectorate under the Danish Ministry of Justice. Three male, Sprague-Dawley rats were implanted by  $4 \times 4$  arrays of 100  $\mu\text{m}$ , length = 2-3 cm tungsten wires spaced 500  $\mu\text{m}$  apart. A craniotomy was performed over the primary motor cortex (M1). The area related to forelimb movement is located 2-4 mm rostral and 2-4 mm lateral relative to Bregma. Layer V and VI were selected and the target depth was at approx. 1.7-1.8 mm. The implantation and surgical procedure is similar to that described previously [38]. Analog neural data were filtered at 400 Hz and 10 kHz before digitization at 24 kHz.

To perform an evaluation of the algorithm using recorded neural cortical data, five data segments were selected for manual detection by the experts. The data segments were manually inspected to provide the ground truth. Each segment of data contained at least 100 spikes identified as true neural waveforms. The marked data were used to compare the detection performance of different methods.

### B. Simulations

The proposed method was tested in 7 sets of simulated signals. For simulating multi-unit neural APs, a library of 21 experimental APs (64 samples per AP) from 3 implanted rats was generated. For simulating neural recordings in each dataset, data segments with length of 2.5 s (60032 samples at sampling rate of 24 kHz) were generated as following. Three spikes were selected from the library and each was distributed randomly in time with average firing rate of 20 Hz. Overlapping between different units was excluded from the simulations in order to eliminate the confounding factor of non-classified overlapped APs when testing and comparing the proposed method. Each data segment contained 150 spikes on average. The background noise was simulated as a colored noise with similar power spectrum as in the experimental recordings. For this purpose, the noise was simulated by an auto-regressive (AR) model which was previously reported to accurately represent the noise in neural recordings [8]. In the simulations, the SNR was defined as:

<sup>1</sup> Reducing the dimension of the feature space by principal component analysis (PCA) was also tested but it did not improve the clustering performance significantly. Thus, PCA was not used for the results reported.



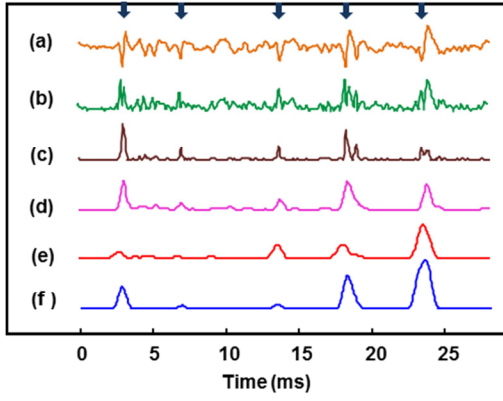


Fig. 3. Visual comparison of the detector output quality for all methods. (a) A section of a band-pass filtered intra-cortical data (recorded as described in section III-A) with the arrows indicating the true time of occurrence for the APs, SNR=1.5. (b) Absolute value waveform used for THR detector. (c) NEO detector waveform. (d) MTEO detector waveform. (e) DWT product detector waveform. (f) Proposed manifestation variable for detection.

$$SNR = \frac{\text{Average of absolute peak amplitude of APs}}{3 \times \text{RMS value of pure noise segment}} \quad (14)$$

The definitions of SNR in previous works on AP detection are several, without an accepted common definition [8, 13, 22, 23]. The definition used in this study [Eq. (14)] does not depend on the level of activity (number of spikes) and is intuitively related to the complexity of detection. For example, SNR=1 represents the situation in which spikes and noise have comparable amplitude levels. According to the proposed SNR definition, 7 levels of added noise were investigated, corresponding to SNR from 1 to 2.5, with increments of 0.25. For each noise level, 20 noise realizations were generated. Before SNR calculation, all simulated signals were band-pass filtered by a fourth-order zero phase-shift butterworth filter (300–6000 Hz).

### C. Performance Measures

Recalling the definition of the detection error rate (DER) as the summation of the two types of errors divided by the total number of spikes [Eq. (10)], the detection performance rate (DPR) was defined by subtracting DER from 100%, which can be also described as the difference between the true positive rate (TPR) and the false positive rate (FPR):

$$DPR = 100\% - DER = \frac{TP - FP}{\text{Spike Number}} \% = TPR - FPR \quad (15)$$

The correct classification rate (CCR) was defined as the percentage of correctly clustered (CC) spikes divided by the total number of spikes:

$$CCR = \frac{CC}{\text{Spike Number}} \% \quad (16)$$

The defined CCR clearly measures the overall classification performance which is influenced by both the detection and clustering performance.

### D. Compared Methods

The proposed method for detection was compared to four commonly used detectors: absolute value thresholding (THR) [6], NEO [14], MTEO [17], and the point-wise product of the wavelet scales described by Kim & Kim [8] (DWT product).

The NEO detector output  $T(n)$  was defined as in [14]:

$$T(n) = x^2(n) - x(n+1) \cdot x(n-1) \quad (17)$$

where  $x(n)$  is sample of the waveform at time  $n$ .

The MTEO detector is an unsupervised combination of the outputs of a few NEOs with different resolution parameters. In this study 1, 3, and 5 are selected as the resolution parameters. The complete method has been described in [17].

The DWT product detector output was defined as in [8]:

$$T(n) = \omega(n) * \left( \prod_{j=j_{\max}-2}^{j_{\max}} |W(2^j, n)| \right) \quad (18)$$

where  $W(2^j, n)$  denotes the wavelet coefficients at scale  $j$ , and  $j_{\max}$  is the scale where the absolute value yields a maximum over 5 dyadic scales. The product absolute value is smoothed by convolution with the Bartlett window  $\omega(n)$ . The Symlet4 as well as an optimized wavelet using the same criterion as for the proposed approach were used as mother wavelet for the DWT product method.

For evaluating the performance of various spike detection methods, the receiver operator characteristic (ROC) curves were used to eliminate the dependence of the comparison to the thresholds. The ROC curves were generated by measuring the relative values of TPR and FPR obtained from applying different threshold levels to the detector outputs.

To evaluate the performance of the detection methods on the complete simulation dataset, an automatic threshold level estimation was used. For the THR method, the automatic threshold level ( $Thr$ ) was set as previously proposed [6]:

$$Thr = 4 \cdot \text{median} \left( \frac{|x|}{0.6745} \right) \quad (19)$$

where  $x$  is the waveform (including the spikes and background noise). The threshold level for NEO, MTEO and DWT product was estimated as a scaled version of the median for absolute value of the detector output:

$$Thr = K \cdot \text{median}(|T(n)|) \quad (20)$$

where  $T(n)$  is the detector output waveform, and  $K$  is a fixed scale. The scale factor  $K$  was selected empirically from the resulting ROC curves of each method after applying simulated signals so that the false positive detection rate was limited to relatively low values (FPR < 10%). The selected  $K$  values were 10, 18, and 8 for the DWT product, NEO, and MTEO methods, respectively.

The proposed wavelet selection criterion was compared to the selection criterion which was recently proposed by Kamavuako et al. [25]. In that study, the detected candidates of APs after wavelet denoising were synchronized and the root mean square of the synchronized average (RMSSA) was the criterion for selection of the optimal wavelet (details can be found in [25]). To compare the performance of the wavelet selection, a two sample  $t$ -test was used to calculate  $p$ -values.

Finally, the clustering results were compared to the Wave\_clus algorithm [6] based on superparamagnetic clustering (SPC). The simulated datasets applied to the software and results were used for measuring the classification performance.

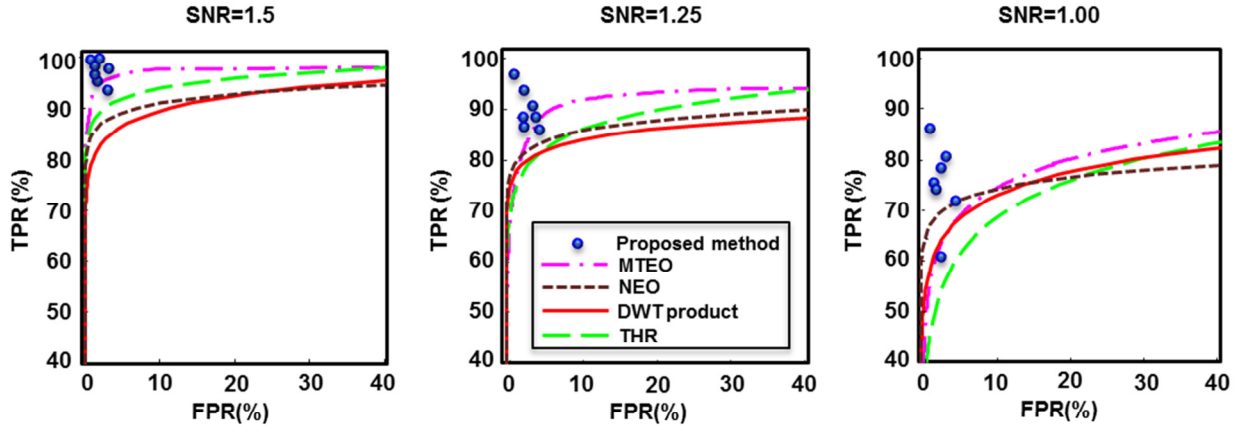


Fig. 4. Comparison of different detection method performance by the averages of ROC curves over 7 simulated signals for three SNR values: 1.5, 1.25, and 1 (indicated at the top of each panel). The horizontal axis of each panel represents the percentage rate of false positives (FPR) and the vertical axis represents the percentage rate of true positives (TPR). The detection methods compared are: the proposed method (circles; one circle for each simulated signal), MTEO (dash point line), NEO (short dash line), DWT product (solid line), and THR (long dash line). The ROC curves presented are averages over the 7 simulated signals.

#### IV. RESULTS

##### A. Simulated Data

###### 1) Detection without Wavelet Optimization

Fig. 3 provides a visual comparison of the detector output quality for all methods tested in this study. The methods were applied on an experimental data segment (of SNR=1.5) in which the APs were manually marked by the experts. The Symlet4 was used as mother wavelet for both the DWT product and the proposed method. The proposed detector output shows clear peaks only at the occurrence times of the APs. Contrarily, other detectors have more spurious peaks.

To compare the detection performance of the proposed method with other four methods of DWT product, MTEO, NEO, and THR, regardless of the effect of the threshold level setting, the ROC curves were computed for three SNRs (1.5, 1.25, and 1). Fig. 4 shows the resulting averages of the ROC curves over 7 simulated signals (each of 10 s length). The

Symlet4 was used as the mother wavelet for the DWT product and for the proposed method. The proposed method is represented by 7 single points (circles) related to 7 signals instead of an average curve since no threshold level was used in the method. The proposed method outperformed the other methods. It is also shown in the figure that the proposed method is robust and resistant to the false positives.

The proposed detection method was evaluated and compared with the DWT product detection method. The comparison was done for three catalogue mother wavelets (Symlet4, Coiflet4, and Daubechies4). Fig. 5 shows the average performance over all independent simulated datasets for the two algorithms. The proposed method outperformed the previous ones in all cases.

###### 2) Detection with Wavelet Optimization

The ideal optimization was defined as the one maximizing the performance by selecting the best mother wavelet in each time segment. The worst optimization was defined as the one

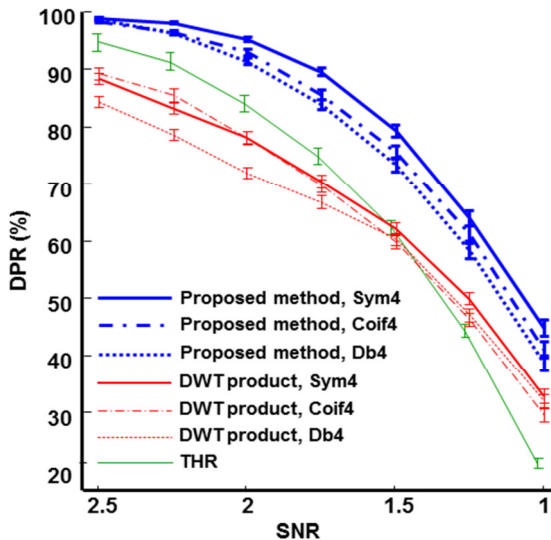


Fig. 5. Average detection performance over all simulated datasets as a function of SNR. The proposed method is compared to the DWT product method for three catalogue mother wavelets (Symlet4, Coiflet4 and Daubechies4) and THR method. DPR: Detection performance rate.

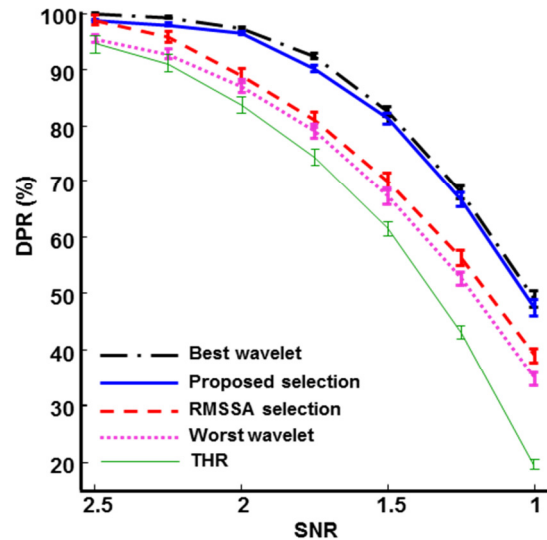


Fig. 6. Average detection performance over the simulated dataset as a function of SNR. The proposed optimal selection is compared to the best wavelet, the RMSSA criterion for selection, the worst wavelet, and THR method. DPR: Detection performance rate.



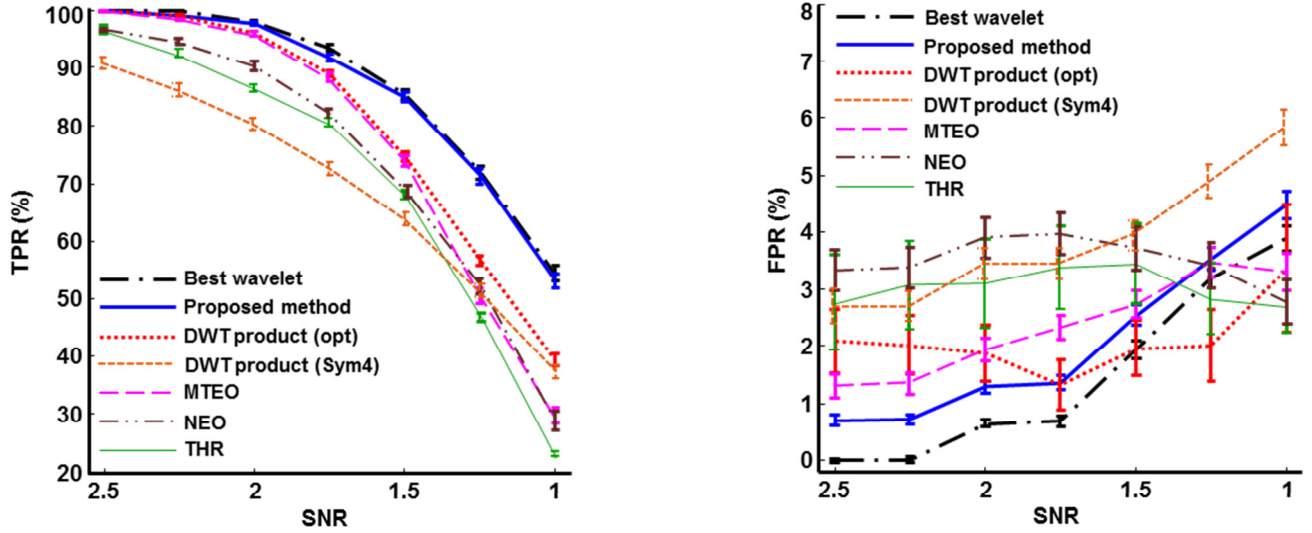


Fig. 7. Comparison of average true positive rates (TPR) in the left panel and average false positive rates (FPR) in the right panel over all simulated datasets versus SNR among all method. The proposed detection method with maximum performance (best wavelet) and unsupervised wavelet selection are compared to the other methods including MTEO, NEO, THR and optimized DWT product method (i.e. with wavelet selection).

that minimized the performance measure. Fig. 6 shows the average a posteriori detection performance for the proposed selection method and for the RMSSA based selection method [25], over all the simulated dataset. The performance of the proposed wavelet selection criterion was close to the ideal optimization. A two sample  $t$ -test was applied to the results of each SNR separately and showed that the performance of the selected wavelet using the proposed criterion was significantly higher than both RMSSA based selection performance ( $p \ll 0.001$ ) and worst optimization performance ( $p \ll 0.001$ ) for all SNRs, whereas the proposed selection performance for SNRs  $\leq 1.5$  was not significantly different from the ideal optimization performance ( $p > 0.2$ ).

A further comparison of detection performance was made between the proposed method after wavelet optimization and the other methods. For the DWT product method, the detection performance was measured both by using a fixed mother wavelet (Symlet4) and by applying the proposed optimization procedure (i.e., wavelet selection). For this comparison the detection rates of true positives (TPR) and false positives (FPR) were used for description of the results instead of the detection performance rate (DPR). In such a way the effect of empirically selected  $K$  scale factor in (20) on false positive detection rates can be studied. Fig. 7 shows this comparison for the average detection results in terms of true positive and false positive detection rates over the simulated dataset. The TPR with the proposed selection criterion are close to the ideal optimization. A two sample  $t$ -test applied to the results of each SNR separately, showed that the TPR of selected wavelet using the proposed criterion was not significantly different from the ideal optimization TPR ( $p > 0.1$ ) for all SNRs. It is also shown in Fig. 7 that the threshold adjustment for all four detection methods had reasonable results of keeping FPR low for the simulated signals and all SNRs. The results indicate that the proposed method outperformed the previous ones in all cases in terms of

TPR, while the FPRs for all methods were kept in the same range. Fig. 7 also indicates that applying the proposed wavelet optimization with the DWT product method substantially improved the detection performance of that method. For SNRs  $\geq 1.5$ , the MTEO outperformed the NEO, THR and non-optimized DWT product methods, whereas the optimized version of the DWT product method outperformed the MTEO for all SNRs.

### 3) Classification

The correct classification rate (CCR) was compared in case of the proposed optimization for clustering and when using the same optimization as used for detection. The ideal (worst) optimization was defined as the one that maximized (minimized) the performance measure by selection of the best (worst) mother wavelet in every time segment. In addition, the proposed method was compared to the Wave\_clus algorithm

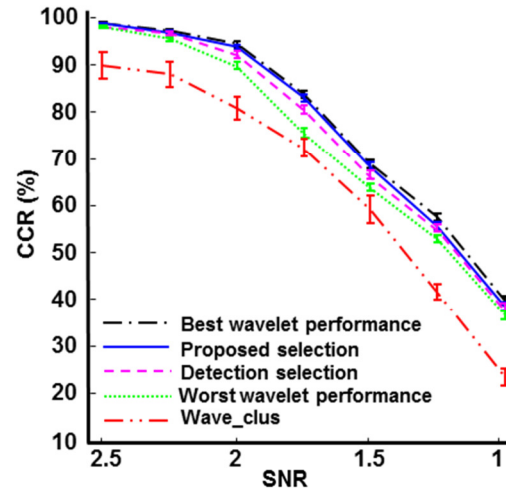


Fig. 8. Comparison of average correct classification rates (CCR) over all simulated datasets versus SNR for all methods. The proposed methods with different wavelet selections in the clustering task (best wavelet performance, proposed criterion for clustering, old criterion for detection and the worst wavelet performance) are compared to the Wave\_clus algorithm.

TABLE I

DETECTION PERFORMANCE RATE (IN PERCENT) OBTAINED BY APPLYING THE SIX ALGORITHMS ON THE EXPERIMENTAL RECORDING SEGMENTS.

Method	THR	DWT product (opt)	NEO	MTEO	Proposed method
Data					
Segment 1	32.9 %	53.1 %	71.1 %	49.2 %	79.2 %
Segment 2	47.8 %	71.0 %	70.3 %	59.3 %	90.1 %
Segment 3	49.0 %	61.5 %	65.6 %	57.5 %	75.6 %
Segment 4	60.3 %	81.1 %	77.6 %	72.8 %	81.1 %
Segment 5	54.1 %	70.4 %	70.6 %	70.4 %	75.2 %
Mean	48.8 %	67.6 %	71.0 %	61.8 %	80.2 %
St. Dev.	10.2 %	10.7 %	4.3 %	9.7 %	6.0 %

[6], which is based on superparamagnetic clustering (SPC). Fig. 8 represents the classification results for all compared cases. The CCR results of the proposed selection criterion are close to the ideal optimization. A two sample  $t$ -test applied to the results of each SNR separately, showed that the CCR of the selected wavelet using proposed criterion was not significantly different from the ideal optimization CCR ( $p > 0.1$ ) for all SNRs whereas the CCR was lower than the ideal value when using the same wavelets as used for detection when the SNR was between 1.5 and 2 ( $p < 0.05$ ). The results indicate that updating the wavelet selection for the clustering task results in better performance than keeping it unchanged from the detection stage. It is also shown in Fig. 8 that the proposed method outperformed the Wave\_clus algorithm in all cases.

#### B. Experimental Data

Table I reports the comparison of detection performance for different detection methods on each segment from experimental recordings. The average SNR of the data segments was 1.48 ( $\pm 0.04$  SD). The results indicate that the proposed method outperformed all other methods tested,

Fig. 9 shows an example of efficiency verification of the proposed criterion for wavelet selection in the detection task on real experimental data (segment 1). The variation of the proposed selection criterion (the number of reference APs in Eq. (12)) versus the parameter  $\alpha$  (representing different mother wavelets) and the corresponding detection results for the experimental data are shown. In this example, the maximum value of the criterion (indicated with the arrows) corresponds to the maximum TPR and the minimum FPR. It is shown in Fig. 9 that the proposed criterion has positive correlation to the TPR and negative correlation to FPR.

### V. DISCUSSION AND CONCLUSION

We have proposed a novel method for unsupervised and automatic detection of APs in extracellular recordings. The denoised wavelet coefficients over selected scales were combined to define a new manifestation variable for detection. In addition, we have proposed two signal-based criteria for unsupervised wavelet basis selection, one to improve the detection performance and the other to improve the classification performance.

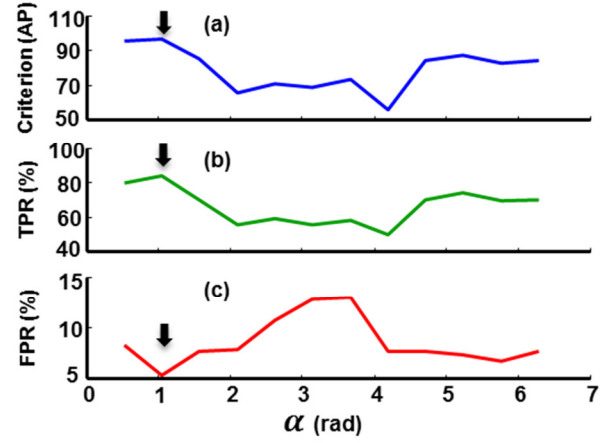


Fig. 9. A comparison of the proposed wavelet selection criterion with the measured detection performance on experimental data. (a) Number of reference APs (proposed signal-based criterion) versus the parameter  $\alpha$ . (b) True positive detection rate (TPR) versus  $\alpha$ . (c) False positive detection rate (FPR) versus  $\alpha$ . The arrows indicate the selected wavelet corresponding to the maximum of the proposed criterion, maximum TPR, and minimum FPR.

#### A. Manifestation Variable for Detecting APs

With respect to other detection methods, the manifestation variable proposed in this study is smoother and less noisy, and consequently more robust against the non-spike events (see Fig. 3). Other detection methods always require threshold level setting for the detector output. Recall from section I that the automatic identification of the threshold level needs prior knowledge on the noise amplitude distribution. Moreover, the comparison of ROC curves for simulated data showed the superiority of the proposed manifestation variable with respect to the previous methods (Fig. 4). The results from this study showed that the proposed technique for combining the information (i.e., the summation of absolute coefficients after denoising) over the selected maximum energy scales can highly improve the detection performance with respect to the DWT point-wise product technique described previously [8] (see Fig. 5). In fact, the DWT product acts like an intersect operator which only takes the common information from the scales, whereas the proposed method acts like a union operator which effectively combines the filtered information from the scales.

#### B. Unsupervised Wavelet Basis Optimization for the Detector and Classifier

As a basic limitation of template matching in detection and classification, the performance relies on a priori knowledge of the spike shape to form the template. This issue has been discussed previously [16, 23]. In a similar way, the performance of wavelet-based methods can be strongly affected by the choice of the mother wavelet shape. This fact, however, has not received much attention in most of the previous wavelet-based methods. In the present study we used a known framework for parameterizing wavelet filter coefficients, as previously applied in many biomedical signal processing applications [25-28]. We proposed a new unsupervised criterion for the optimization based on correlation measures on the detected APs. The *a posteriori*

performance measurement for all simulated datasets showed that the proposed criterion optimized the wavelet selection quite efficiently (with respect to minimum and maximum performance) for the detection task (Fig. 6) and significantly outperformed the optimization results obtained by a criterion previously proposed (RMSSA) [25]. The reason for this result is that the RMSSA criterion only measures the average power of the detected spikes which is independent to the number of detections. Consequently it is not sensitive to the type II errors (missed APs) which are common in low SNR conditions, as those studied in this work.

The results obtained from the simulation study showed that the TPR index for the proposed method using unsupervised wavelet selection was not significantly different from that of the ideal optimization and was substantially higher than other previous detection methods whereas the FPR for all methods was in the same range (Fig. 7). Among the previous detection methods, the optimized DWT product method showed superior performance in the SNR range studied for the simulated dataset (Fig. 7). These results show that the wavelet based methods outperformed the other compared methods when an appropriate wavelet selection was used.

Since the DWT coefficients are used as the primary features in the clustering task, the classification performance could be influenced by basis selection of the wavelet. To study this relation, we have proposed another algorithm for the wavelet optimization in the clustering task by defining a new criterion to improve the separability of the clusters. The obtained results from the simulated dataset showed that the classification performance depends on the selection of the mother wavelet and updating the wavelet selection for the clustering task using the proposed criterion can lead to higher performance than keeping it unchanged from the detection stage (Fig. 8). Moreover, the classification performance of the proposed method was higher than with the Wave\_clus algorithm [6] based on superparamagnetic clustering.

### C. Methodological Considerations

The colored noise which we used in the simulations reproduces the frequency content of a realistic background noise, while it does not necessarily reproduce the time domain characteristics of the experimental noise. This may be considered as a potential limitation. However, with the exception of the THR detector which is based on amplitude thresholding in the time domain, all other detectors and sorters, including the NEO, MTEO, DWT product, SPC, and the proposed method, are based on both frequency and time domain characteristics. Thus, the frequency content of the simulated noise is very relevant for the performance. Moreover, all methods have been compared under the same conditions (simulations), thus the comparison among methods remains unbiased.

We would like also to point out that we have used a limited set of experimental signals only to verify the results obtained from the simulated datasets. The realistic simulation enabled us to cover a wider range of conditions in the test signals and

to provide more accurate quantitative evaluation (for example, sensitivity to various noise levels).

The computational cost for the proposed algorithm is higher than the classic detection algorithms, such as THR, MTEO or NEO. This may be considered as a limitation for this algorithm at first glance. However, the accurate number of floating point arithmetic operations for execution of non-optimized MATLAB codes for the THR detector and the proposed detector (without optimization) for detecting APs in a data segment of 1 s were calculated as 3.87 and 17.83 millions respectively. This means that the proposed detector would be acceptable for online BCI applications with normal PCs. The wavelet optimization process, which is more time consuming, can be updated occasionally (e.g., every 10 s).

In conclusion, the results of this study show that the newly defined manifestation variable can be used as a powerful and robust technique for action potential detection with acceptable computational cost for online implementation. Moreover, it was shown that the proposed signal-based criteria for the optimization of the mother wavelet substantially improved both detection and classification performance, by eliminating the dependence of the methods to the choice of the mother wavelet. The proposed unsupervised optimization can be applied potentially to any wavelet-based method for the purpose of spike detection and sorting.

### ACKNOWLEDGMENT

The authors would like to thank S.H.H. Hammad, for his help in recording experimental neural signals.

### REFERENCES

- [1] J. K. Chapin, K. A. Moxon, R. S. Markowitz and M. A. Nicolelis, "Real-time control of a robot arm using simultaneously recorded neurons in the motor cortex," *Nat. Neurosci.*, vol. 2, pp. 664-670, Jul, 1999.
- [2] L. R. Hochberg, M. D. Serruya, G. M. Friehs, J. A. Mukand, M. Saleh, A. H. Caplan, A. Branner, D. Chen, R. D. Penn and J. P. Donoghue, "Neuronal ensemble control of prosthetic devices by a human with tetraplegia," *Nature*, vol. 442, pp. 164, 2006.
- [3] M. S. Lewicki, "A review of methods for spike sorting: the detection and classification of neural action potentials," *Network*, vol. 9, pp. R53-78, Nov, 1998.
- [4] I. N. Bankman and S. J. Janselewitz, "Neural waveform detector for prosthesis control," in *Proc. 17th Ann. Conf. IEEE EMBS*, 1995, pp. 963-964.
- [5] R. Chandra and L. Optican, "Detection, classification, and superposition resolution of action potentials in multiunit single-channel recordings by an on-line real-time neural network," *IEEE Trans. Biomed. Eng.*, vol. 44, pp. 403-412, 1997.
- [6] R. Q. Quiroga, Z. Nadasdy and Y. Ben-Shaul, "Unsupervised spike detection and sorting with wavelets and superparamagnetic clustering," *Neural Comput.*, vol. 16, pp. 1661-1687, 2004.
- [7] M. S. Fee, P. P. Mitra and D. Kleinfeld, "Variability of extracellular spike waveforms of cortical neurons," *J. Neurophysiol.*, vol. 76, pp. 3823-3833, Dec, 1996.
- [8] K. H. Kim and S. J. Kim, "A wavelet-based method for action potential detection from extracellular neural signal recording with low signal-to-noise ratio," *IEEE Trans. Biomed. Eng.*, vol. 50, pp. 999, Aug, 2003.
- [9] F. Worgotter, W. J. Daunicht and R. Eckmiller, "An on-line spike form discriminator for extracellular recordings based on an analog correlation technique," *J. Neurosci. Methods*, vol. 17, pp. 141-151, 1986.
- [10] H. Kaneko, S. S. Suzuki, J. Okada and M. Akamatsu, "Multineuronal spike classification based on multisite electrode recording, whole-waveform analysis, and hierarchical clustering," *IEEE Trans. Biomed. Eng.*, vol. 46, pp. 280-290, Mar, 1999.

- [11] S. N. Gozani, "Optimal discrimination and classification of neuronal action potential waveforms from multiunit, multichannel recordings using software-based linear filters," *IEEE Trans. Biomed. Eng.*, vol. 41, pp. 358, 1994.
- [12] P. M. Zhang, J. Y. Wu, Y. Zhou, P. J. Liang and J. Q. Yuan, "Spike sorting based on automatic template reconstruction with a partial solution to the overlapping problem," *J. Neurosci. Methods*, vol. 135, pp. 55-65, May 30, 2004.
- [13] S. Kim and J. McNames, "Automatic spike detection based on adaptive template matching for extracellular neural recordings," *J. Neurosci. Methods*, vol. 165, pp. 165-174, Sep 30, 2007.
- [14] K. H. Kim and S. J. Kim, "Neural spike sorting under nearly 0-dB signal-to-noise ratio using nonlinear energy operator and artificial neural-network classifier," *IEEE Trans. Biomed. Eng.*, vol. 47, pp. 1406-1411, Oct. 2000.
- [15] S. Mukhopadhyay and G. C. Ray, "A new interpretation of nonlinear energy operator and its efficacy in spike detection," *IEEE Trans. Biomed. Eng.*, vol. 45, pp. 180-187, Feb, 1998.
- [16] I. Obeid and P. D. Wolf, "Evaluation of spike-detection algorithms for a brain-machine interface application," *IEEE Trans. Biomed. Eng.*, vol. 51, pp. 905-911, Jun, 2004.
- [17] J. H. Choi, H. K. Jung and T. Kim, "A new action potential detector using the MTEO and its effects on spike sorting systems at low signal-to-noise ratios," *IEEE Trans. Biomed. Eng.*, vol. 53, pp. 738-746, 2006.
- [18] I. Obeid, "Comparison of spike detectors based on simultaneous intracellular and extracellular recordings," in *Proc. 3rd Int. IEEE/EMBS Conf. Neural Eng.* 2007, pp. 410-413.
- [19] S. Gibson, J. W. Judy and D. Markovic, "Comparison of spike-sorting algorithms for future hardware implementation," *Proc. 30th Ann. Int. Conf. IEEE EMBS*, pp. 5015-5020, 2008.
- [20] K. G. Oweiss and D. J. Anderson, "Noise reduction in multichannel neural recordings using a new array wavelet denoising algorithm," *Neurocomputing*, vol. 38, pp. 1687, 2001.
- [21] E. Hulata, R. Segev and E. Ben-Jacob, "A method for spike sorting and detection based on wavelet packets and Shannon's mutual information," *J. Neurosci. Methods*, vol. 117, pp. 1-12, 30 May, 2002.
- [22] A. Diedrich, W. Charoensuk, R. J. Brychta, A. C. Ertl and R. Shiavi, "Analysis of raw microneurographic recordings based on wavelet denoising technique and classification algorithm: wavelet analysis in microneurography," *IEEE Trans. Biomed. Eng.*, vol.50, pp. 41-50, 2003.
- [23] Z. Nenadic and J. W. Burdick, "Spike detection using the continuous wavelet transform," *IEEE Trans. Biomed. Eng.*, vol.52, pp. 74-87, 2005.
- [24] C. Gold, D. A. Henze, C. Koch and G. Buzsáki, "On the origin of the extracellular action potential waveform: a modeling study," *J. Neurophysiol.*, vol. 95, pp. 3113, 2006.
- [25] E. N. Kamavuoko, W. Jensen, K. Yoshida, M. Kurstjens and D. Farina, "A criterion for signal-based selection of wavelets for denoising intrafascicular nerve recordings," *J. Neurosci. Methods*, vol. 186, pp. 274-280, 2010.
- [26] D. Farina, O. F. Nascimento, M. F. Lucas and C. Doncarli, "Optimization of wavelets for classification of movement-related cortical potentials generated by variation of force-related parameters," *J. Neurosci. Methods*, vol. 162, pp. 357-363, 2007.
- [27] L. Brechet, M. F. Lucas, C. Doncarli and D. Farina, "Compression of biomedical signals with mother wavelet optimization and best-basis wavelet packet selection," *IEEE Trans. Biomed. Eng.*, vol. 54, pp. 2186-2192, 2007.
- [28] D. Farina, M. F. Lucas and C. Doncarli, "Optimized wavelets for blind separation of nonstationary surface myoelectric signals," *IEEE Trans. Biomed. Eng.*, vol. 55, pp. 78-86, 2008.
- [29] W. M. Lawton, "Tight frames of compactly supported affine wavelets," *Journal of Mathematical Physics*, vol. 31, pp. 1898-1901, 1990.
- [30] W. M. Lawton, "Necessary and sufficient conditions for constructing orthonormal wavelet bases," *Journal of Mathematical Physics*, vol. 32, pp. 57-61, 1991.
- [31] D. L. Donoho and I. M. Johnstone, "Ideal spatial adaptation by wavelet shrinkage," *Biometrika*, vol. 81, pp. 425, 1994.
- [32] D. L. Donoho, "De-noising by soft-thresholding," *IEEE Trans. Inf. Theory*, vol. 41, pp. 613-627, 1995.
- [33] S. Mallat and S. Zhong, "Characterization of signals from multiscale edges," *IEEE Trans. Pattern Anal. Mach. Intell.*, vol. 14, pp. 710, 1992.
- [34] Y. Xu and J. B. Weaver, "Wavelet transform domain filters: a spatially selective noise filtration technique," *IEEE Trans. Image Process.*, vol. 3, pp. 747-758, 1994.

- [35] L. Zhang and P. Bao, "Edge detection by scale multiplication in wavelet domain," *Pattern Recog. Lett.*, vol. 23, pp. 1771, 2002.
- [36] J. H. Ward Jr, "Hierarchical grouping to optimize an objective function," *J. American Stat. Assoc.*, vol. 58, pp. 236-244, 1963.
- [37] G. W. Milligan and P. D. Isaac, "The validation of four ultrametric clustering algorithms," *Pattern Recognition*, vol. 12, pp. 41-50, 1980.
- [38] W. Jensen and P. J. Rousche, "Encoding of self-paced, repetitive forelimb movements in rat primary motor cortex," in *Proc. 26th Ann. Int. Conf. IEEE EMBS*, 2004, pp. 4233-4236.



**Vahid Shalchyan** (S'12) received the B.Sc. degree in electrical engineering from the University of Tehran, Tehran, Iran, in 1998, and the M.Sc. degrees in biomedical engineering from Amirkabir University of Technology, Tehran, Iran, in 2002. He is currently undertaking his Ph.D. degree at The International Doctoral School in Biomedical Science and Engineering, Aalborg University, Aalborg, Denmark. Since 2011, He has been a visiting researcher at the Department of Neurorehabilitation Engineering at the University Medical Center Göttingen, Georg-August University, Germany. His main research interests include biomedical signal processing and pattern recognition, with emphasis on their application to neural signals, for neuroscience, neurotechnology, and brain-computer interface researches.



**Winnie Jensen** (M'8) received her Master of Science degree in electrical engineering in 1997 and her Ph.D. degree in bioengineering in 2001 from Dept. Health Science and Technology at Aalborg University, Denmark. From 2003 to 2006 she was a Postdoctoral Fellow at the University of Illinois at Chicago, USA. In 2003 she was awarded an EU Marie Curie Outgoing International Fellowship. She has been working as an associate professor at the Dept. Health Science and Technology at Aalborg University, Denmark since 2006. Dr. Jensen is a member of the IEEE and the Society for Neuroscience. Her main research interests include use of implantable neural interfaces in neural prosthesis applications, and the integration of neural prosthesis applications at peripheral and cortical level.



**Dario Farina** (M'01-SM'09) obtained the MSc degree in Electronics Engineering from Politecnico di Torino, Torino, Italy, in 1998, and the PhD degrees in Automatic Control and Computer Science and in Electronics and Communications Engineering from the Ecole Centrale de Nantes, Nantes, France, and Politecnico di Torino, respectively, in 2002. In 2002-2004 he has been Research Assistant Professor at Politecnico di Torino and in 2004-2008 Associate Professor in Biomedical Engineering at Aalborg University, Aalborg, Denmark. From 2008 to 2010 he has been Full Professor in Motor Control and Biomedical Signal Processing and Head of the Research Group on Neural Engineering and Neurophysiology of Movement at Aalborg University. In 2010 he has been appointed Full Professor and Founding Chair of the Department of Neurorehabilitation Engineering at the University Medical Center Göttingen, Georg-August University, Germany, within the Bernstein Center for Computational Neuroscience. He is also the Chair for Neuroinformatics of the Bernstein Focus Neurotechnology Göttingen. Since 2010 he is the Vice-President of the International Society of Electrophysiology and Kinesiology (ISEK). He is the recipient of the 2010 IEEE Engineering in Medicine and Biology Society Early Career Achievement Award for his contributions to biomedical signal processing and to electrophysiology and in 2012 he has been elected Fellow of the American Institute for Medical & Biological Engineering (AIMBE). He is an Associate Editor of Medical & Biological Engineering & Computing and member of the Editorial Boards of the Journal of Electromyography and Kinesiology and of the Journal of Neuroscience Methods. His research focuses on biomedical signal processing, modeling, neurorehabilitation technology, and neural control of movement. Within these areas, he has (co)-authored approximately 250 papers in peer-reviewed Journals and over 300 among conference papers/abstracts, book chapters and encyclopedia contributions. He is an Associate Editor of IEEE TRANSACTIONS ON BIOMEDICAL ENGINEERING.